

Supporting Information

Article title: **Sexual modulation in a polyploid grass: a reproductive contest between environmentally inducible sexual and genetically dominant apomictic pathways**

Authors: Piyal Karunaratne^{1,2*}, Anna V. Reutemann³, Mara Schedler³, Adriana Glücksberg³, Eric J. Martínez³, Ana I. Honfi⁴, and Diego H. Hojsgaard¹

The following Supporting Information is available for this article:

Figure S1. Overall trend of the observed reproductive potential x reproductive efficiency values for each reproductive pathway plotted against MDR zones. **a:** apomixis; **b:** sexuality.

Figure S2. Plot depicting the nonlinear curve fitting of mean functions explaining the observed response of meiotic and apomictic embryo sacs proportions under different MDR.

Figure S3. Response of sexual reproductive efficiency from populations sharing similar sexual reproductive potential located under different MDR zones.

Table S1. All the studied populations of *Paspalum intermedium* in the study, including locations, geographic coordinates and voucher codes.

Table S2. Proportion of sexual (meiotic) and apomictic reproductive pathways in ovules at blooming (mature embryo sacs) and seed stages of the studied *P. intermedium* populations.

Table S3. Reproductive pathways fitness analysis of the studied *P. intermedium* populations

Table S4. Pearson correlation of meiotic (r_{sex}) and apomictic (r_{apo}) proportions at ovule and seed stages to different climatic variables.

Table S5. Proportion of sexual (meiotic) and apomictic reproductive pathways in *P. intermedium* populations under different MDR zones.

Methods S1 Nonlinear function explaining environmental influence on reproductive pathways

Fig. S1. Overall trend of the observed reproductive potential x reproductive efficiency values for each reproductive pathway plotted against MDR zones. **a:** apomixis; **b:** sexuality.

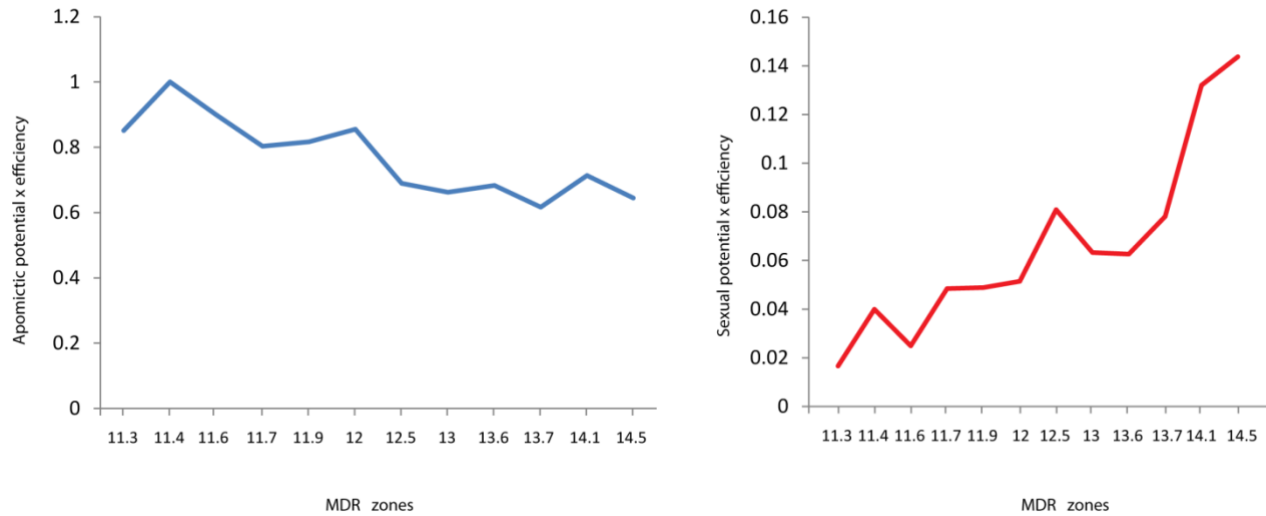


Fig. S2. Plot depicting the nonlinear curve fitting of mean functions explaining the observed response of meiotic and apomictic embryo sacs proportions observed under different mean diurnal ranges in the studied area.

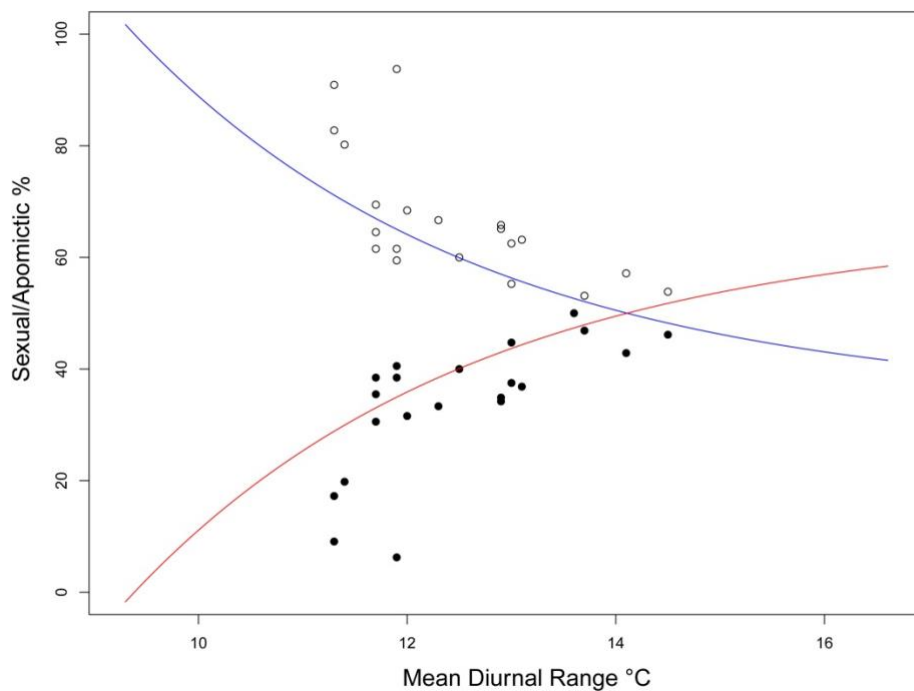


Fig. S3. Response of sexual reproductive efficiency from populations sharing similar sexual reproductive potential located under different MDR zones. **a:** three populations between 11.7°C-12.5°C MDR zones and with 0.41 ± 0.01 sexual potential. **b:** four populations between 11.7°C-13.7°C MDR zones and with 0.53 ± 0.01 sexual potential. **c:** three populations between 11.4°C-14.5°C MDR zones and with 0.65 ± 0.02 sexual potential.

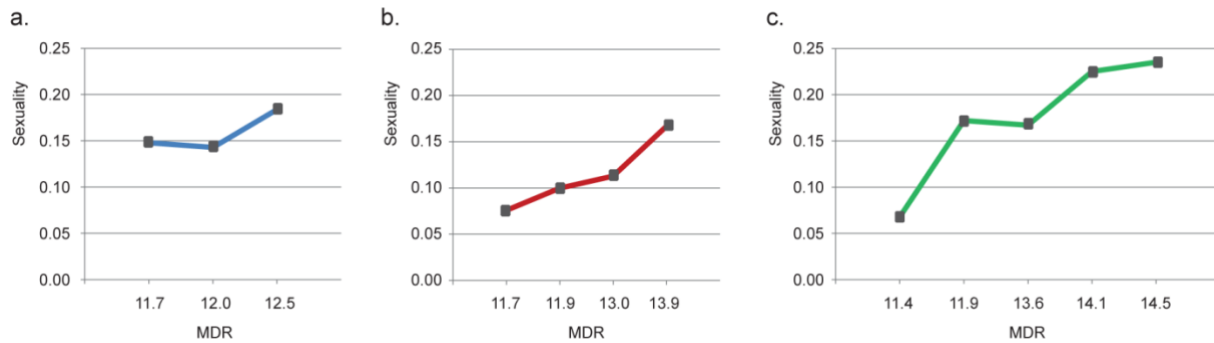


Table S1 All the studied populations of *Paspalum intermedium* in the study, including locations, geographic coordinates and voucher codes.

Col._code	Pop. Label	Longitude	Latitude	Location and vouchers	Ploidy (x=10)
Hojs401	1A	-57.0760	-27.5831	Ctes, NR12, b/ Ituzaingó and Itá Ibaté HojsHonMar401 (CTES, MNES)	4x
M29	1B	-56.8626	-29.4254	Ctes, Dpt Gral San Martín, NR14, 4km South-western PR126 intersection MarSched29 (CTES)	4x
Hojs402	1C	-57.2814	-29.6079	Ctes, PR123, b/access to NR14 Aguapey creek HojsHonMar402 (CTES, MNES)	4x
Hojs403	1D	-57.4844	-29.8267	Ctes, PR126, b/ Curuzú Cuatiá and Paso de los Libres HojsHonMar403 (CTES, MNES)	4x
Hojs404	1E	-58.2093	-29.9081	Ctes, PR126, b/ Curuzú Cuatiá and Sauce HojsHonMar404 (CTES, MNES)	4x
Hojs405	1F	-58.7083	-30.1007	Ctes, Dpt Sauce, PR126, 9 km of Sauce, b/ C.Cuatiá and Sauce HojsHonMar405 (CTES, MNES)	4x
Hojs406	1G	-58.8357	-29.8732	Ctes, Dpt Sauce, PR23, b/ Barrancas'creek and Perugorría HojsHonMar406 (CTES, MNES)	4x

Hoj409	1H	-58.65584	-29.4700	Ctes, Dpt Curuzú Cuatiá, PR23, 16 km from Perugorría HojHonMar409 (CTES, MNES)	4x
Hoj410	1I	-58.65475	-29.2953	Ctes, PR24, b/Perugorría intersection to NR12 HojHonMar410	4x
Hoj414	1J	-59.1137	-27.5268	Chaco, NR11, near Resistencia HojSchedMar414 (CTES, MNES)	4x
Hoj415	1K	-59.34552	-28.4824	Sta Fe, Villa Ocampo, NR11 and access to slaughterhouse HojSchedMar415 (CTES, MNES)	4x
Hoj416	1M	-59.77002	-29.5801	Sta Fe, PR1, 3 km Southern Romang (1 km before El Gusano creek) HojSchedMar416 (CTES, MNES)	4x
Hoj420	1P	-59.63136	-28.5292	Sta Fe, PR32, 5 Km Southern Villa Ana	2x
Hoj422	1Q	-59.61130	-27.0991	Chaco, NR16, 73 km North-eastern from Resistencia HojSchedMar422 (CTES, MNES)	2x
Hoj423	1R	-59.73522	-25.2539	Formosa, NR95, 13 km Eastern Ibarreta	2x
Hoj424	1S	-58.9320	-24.9565	Formosa, NR86, 41 km North-western Espinillo HojSchedMar424 (CTES, MNES)	4x
Hoj425	1T	-58.1383	-25.4033	Formosa, PR6, 15 km Eastern Riacho He He	2x
Hoj429	1U	-58.1427	-25.9639	Formosa, NR11, 25 km Northern Formosa's city	2x
Hoj432	1V	-58.9334	-25.7758	Formosa, NR81, 89 km North-western Formosa's city	2x
M31	1W	-59.2832	-26.0011	Formosa, PR3 MarSched31 (CTES)	2x
M26	1X	-59.3546	-26.2404	Formosa, PR3, 9 km Northern El Colorado town MarSched26 (CTES)	2x
Hoj440	2C	-59.8931	-27.7347	Chaco, PR7, towards La Sabana settlement	4x
Hoj443	2F	-60.0928	-28.7823	Sta Fe, PR3, Southern La Colmena settlement HojKaruSchedMar443 (CTES, MNES)	4x
Hoj445	2H	-60.1769	-29.2907	Sta Fe, PR3, 2,5 Km after Toba asttlement, 21 km Northern Vera HojKaruSchedMar445 (CTES, MNES)	4x

Hoj451	2M	-61.1900	-30.5030	Sta Fe, PR4, 21 km Southern San Cristobar HojKaruSchedMar451 (CTES, MNES)	4x
Hoj453	2Ñ	-61.0815	-29.3140	Sta Fe, PR13, 3-5 km before intersect NR98 towards Chaco HojKaruSchedMar453 (CTES, MNES)	4x
Hoj454	2O	-60.9924	-29.1106	Sta Fe, PR13, 20 km North of NR98 intersection	4x
Hoj455	2P	-60.7479	-28.1586	Sta Fe, PR13, 18 km before the border with Chaco HojKaruSchedMar455 (CTES, MNES)	4x
Hoj456	2Q	-60.6998	-27.4953	Chaco, NR95, 10 km after Villa Angela, towards R.S. Peña HojKaruSchedMar456 (CTES, MNES)	2x, 4x
Hoj465	2R	-60.1767	-26.8977	Chaco, NR16 and intersection to Colonia Aborigen, from R.S. Peña towards Resistencia HojKaruSchedMar465 (CTES, MNES)	4x
Hoj468	2S	-58.7822	-26.8863	Chaco, NR11, 66 km Northern Resistencia HojKaruSchedMar468 (CTES, MNES)	2x
Hoj470	2T	-58.1248	-27.7428	Ctes, PR5, 53 km from San Luis del Palmar towards Caá Catí HojKaruHonMar470 (CTES, MNES)	2x, 3x, 4x
Hoj475	2U	-58.0026	-31.2670	Entre Rios, dirt road on Monseñor Ricardo Rösch Avenue HojKaruHonMar475 (CTES, MNES)	4x
Hoj478	2V	-56.3832	-28.7934	Ctes, NR14, 37 km Northern Alvear town HojKaruHonMar478 (CTES, MNES)	4x
Hoj481	2W	-55.9309	-28.3438	Ctes, PR94, 27 km Northern Santo Tome's city, after PR174 intersection HojKaruMar481 (CTES, MNES)	2x, 4x
Hoj471	2X	-57.9346	-28.3483	Ctes. Rita pcial 6-1 Concepcion a 9 km	4x
Hoj487	2Y	-58.7454	-28.1656	Ctes, NR12, 16 km North-western Saladas, milestone km 951	2x, 4x
M9		-58.3854	-27.6132	Corrientes, PR5, 21 km from San Luis del Palmar towards Caá Cati	2x

Col._Code: collection code; Pop. Label: population label; NR: national route; PR: provincial route; b/: between; Hojs: Hojsgaard D; Sched: Schedler M; Mar: Martínez E; Hon: Honfi A; Karu: Karunaratne P. Acronyms follow the *Index Herbariorum* (Thiers 2017)

Table S2. Proportion of sexual (meiotic) and apomictic reproductive pathways in ovules at blooming (mature embryo sacs) and seed stages of the studied *P. intermedium* populations.

Collection code (label)	ES proportions		Reprod. efficiency		Potential for†		Multiple
	Meiotic	Apomictic	Sexual	Apomictic	Sexuality	Apomixis	AES§
Hoj402(1C)	0.161	0.839	0.981	1.004	0.178	0.857	0.071
Hoj414(1J)	0.046	0.930	0.719	1.029	0.1	1	0.65
Hoj403(1D)	0.304	0.652	0.164	1.594	0.7	1	0.2
Hoj470(2T)	0.654	0.308	0.491	2.072	0.85	0.4	0
Hoj404(1E)	0.294	0.706	0.196	1.507	0.555	0.889	0.222
Hoj409(1H)	0.244	0.755	0.198	1.355	0.367	0.833	0.267
Hoj410(1I)	0.305	0.694	0.74	1.144	0.423	0.769	0.154
Hoj405(1F)	0.385	0.615	0.249	1.503	0.5	0.75	0
Hoj478(2V)	0.043	0.956	0.593	1.027	0.062	0.937	0.437
Hoj471(2X)	0.319	0.617	0.423	1.396	0.6	0.88	0.24
Hoj415(1K)	0.267	0.733	0.45	1.256	0.428	0.928	0.143
Hoj475(2U)	0.385	0.577	0.459	1.361	0.417	0.625	0.0417
Hoj424(1S)	0.349	0.651	0.342	1.397	0.5	0.833	0.1
Hoj445(2H)	0.383	0.596	0.215	1.636	0.567	0.7	0.067
Hoj465(2R)	0.465	0.535	0.152	1.848	0.667	0.667	0.033
Hoj453(2Ñ)	0.375	0.575	0.355	1.569	0.517	0.586	0.207
Hoj455(2P)	0.328	0.641	0.525	1.358	0.7	0.933	0.2
Hoj456(2Q)	0.353	0.529	0.509	1.423	0.6	0.7	0.2

†: the potential for each reproductive pathway includes those ovules with both MES and AES;

§: values for the proportion of ovules carrying more than one AES among total numbers of ovules analyzed per population;

Table S3. Reproductive pathways fitness analysis of the studied *P. intermedium* populations.

Col._code	Pop. Label	Ploidy (x=10)	No. of seed sets (full)/infl.	full seeds (%)	No. of infl./ind.	Germinability	Relative Fitness
Hoj420	1P	2x	3866.8	32.96	45.7	0.781	0.444
Hoj422	1Q	2x	4872.2	37.46	47.0	0.781	0.435
Hoj423	1R	2x	6047.6	25.55	43.7	0.552	0.235
Hoj429	1U	2x	5335.1	24.95	14.3	0.757	0.103
M31	1W	2x	4703.8	46.75	32.7	0.698	0.318
M26	1X	2x	4934.0	29.73	59.7	0.781	0.412
Hoj468	2S	2x	6653.0	21.70	11.0	0.630	0.066
M9		2x	3339.1	40.70	83.3	0.800	0.427
Hoj470	2T	2x, 3x, 4x	2590.0	39.55	8.0	0.710	0.039
Hoj456	2Q	2x, 4x	3255.3	4.10	11.5	0.550	0.006
Hoj481	2W	2x, 4x	3934.4	10.19	14.7	0.829	0.031
Hoj487	2Y	2x, 4x	5563.8	22.33	38.3	0.807	0.388
M29	1B	4x	3910.6	22.86	60.7	0.657	0.267
Hoj402	1C	4x	1475.0	2.85	20.0	0.757	0.004
Hoj403	1D	4x	4984.0	3.03	10.0	0.880	0.009
Hoj404	1E	4x	4305.8	13.07	17.0	0.828	0.051
Hoj405	1F	4x	4123.3	22.35	12.7	0.952	0.074
Hoj406	1G	4x	7598.0	22.49	44.0	0.930	0.499
Hoj409	1H	4x	7486.0	6.51	17.0	0.680	0.039
Hoj410	1I	4x	2645.0	23.63	23.0	0.860	0.086
Hoj414	1J	4x	3021.0	32.03	26.3	0.829	0.135
Hoj416	1M	4x	3156.7	7.03	20.7	0.762	0.063
Hoj424	1S	4x	4387.5	18.69	32.1	0.740	0.128
Hoj440	2C	4x	7038.0	8.38	52.7	0.790	0.129
Hoj443	2F	4x	7129.5	4.81	65.0	0.800	0.126
Hoj453	2Ñ	4x	1549.5	18.63	47.5	0.910	0.120
Hoj465	2R	4x	3198.0	23.96	43.3	0.757	0.160
Hoj475	2U	4x	3161.9	5.53	18.0	0.848	0.019
Hoj471	2X	4x	4825.6	13.26	23.7	0.657	0.059

Col._Code: collection code; Pop. Label: population label.

Table S4. Pearson correlation of meiotic (r_{sex}) and apomictic (r_{apo}) proportions at ovule and seed stages to different climatic variables.

Climatic Variable§	Embryo Sacs			Seeds		
	p-value	r_{apo}	r_{sex}	p-value	r_{apo}	r_{sex}
BIO1:Annual Mean Temperature	0.828	-0.051	0.051	0.989	-0.004	0.004
BIO2 : Mean Diurnal Range†	0.000	-0.699	0.679	0.030	-0.523	0.559
BIO3 : Isothermality (BIO2/BIO7) (* 100)	0.042	-0.447	0.447	0.691	-0.112	0.112
BIO4 : Temperature Seasonality (st. dev. *100)	0.281	-0.247	0.247	0.223	-0.334	0.334
BIO5 : Max Temperature of Warmest Month	0.023	-0.306	0.306	0.083	-0.462	0.462
BIO6 : Min Temperature of Coldest Month	0.074	0.399	-0.399	0.174	0.371	-0.371
BIO7 : Temperature Annual Range (BIO5- BIO6)	0.001	-0.686	0.686	0.054	-0.379	0.379
BIO8 : Mean Temperature of Wettest Quarter	0.037	-0.452	0.458	0.068	-0.365	0.325
BIO9 : Mean Temperature of Driest Quarter	0.939	0.018	-0.018	0.766	0.084	-0.084
BIO10 : Mean Temperature of Warmest Quarter	0.523	-0.148	0.148	0.619	-0.140	0.140
BIO11 : Mean Temperature of Coldest Quarter	0.939	0.018	-0.018	0.766	0.084	-0.084
BIO12 : Annual Precipitation	0.090	0.178	-0.178	0.115	0.424	-0.424
BIO13 : Precipitation of Wettest Month	0.052	0.417	-0.407	0.796	-0.073	0.073
BIO14 : Precipitation of Driest Month	0.061	0.386	-0.386	0.048	0.518	-0.518
BIO15 : Precipitation Seasonality (CV)	0.004	-0.605	0.605	0.051	-0.332	0.332
BIO16 : Precipitation of Wettest Quarter	0.005	0.591	-0.591	0.698	0.109	-0.109
BIO17 : Precipitation of Driest Quarter	0.001	0.668	-0.668	0.077	0.370	-0.370
BIO18 : Precipitation of Warmest Quarter	0.648	0.106	-0.106	0.295	-0.289	0.289
BIO19 : Precipitation of Coldest Quarter	0.001	0.668	-0.668	0.077	0.370	-0.370
UV-B Radiation	0.388	-0.199	0.199	0.567	-0.161	0.161
Elevation	0.508	-0.153	0.153	0.414	0.228	-0.228
Photosynthetically Active Radiation (PAR)	0.925	0.022	-0.022	0.708	0.106	-0.106
Cloud Cover (%)	0.069	0.275	-0.263	0.233	0.328	-0.328
Frost Day Frequency (no. of days)	0.102	-0.367	0.367	0.536	-0.174	0.174
Vapor pressure at ground level	0.663	0.101	-0.101	0.475	0.200	-0.200

§: Bioclimatic variables are as in WorlClim data base; †: Mean of monthly diurnal temperature range (max temp - min temp);

Table S5. Proportion of sexual (meiotic) and apomictic reproductive pathways in *P. intermedium* populations under different MDR zones.

Col. Code (pop. label)	Condition	Bio2 (MDR)	Sexual	Apomictic
Hoj402(1C)	natural	11.3	0.169	0.831
Hoj414(1J)	natural	11.3	0.067	0.933
Hoj403(1D)	natural	11.4	0.068	0.932
Hoj470(2T)	natural	11.6	0.333	0.667
Hoj404(1E)	natural	11.7	0.076	0.924
Hoj409(1H)	natural	11.7	0.061	0.939
Hoj410(1I)	natural	11.7	0.263	0.737
Hoj405(1F)	natural	11.9	0.1	0.9
Hoj478(2V)	natural	11.9	0.037	0.963
Hoj471(2X)	natural	11.9	0.172	0.828
Hoj415(1K)	natural	12	0.143	0.857
Hoj475(2U)	natural	12.5	0.184	0.816
Hoj424(1S)	natural	13	0.129	0.871
Hoj445(2H)	natural	13	0.096	0.904
Hoj465(2R)	natural	13.6	0.076	0.924
Hoj453(2Ñ)	natural	13.7	0.167	0.833
Hoj455(2P)	natural	14.1	0.225	0.775
Hoj456(2Q)	natural	14.5	0.235	0.765
Hoj414(J15)	cultivated	11.1	0.0	1.0
Hoj414(J8)	cultivated	11.1	0.077	0.923
Hoj445 (2H)	cultivated	11.1	0.0	1.0
Hoj404(E4)	cultivated	11.1	0.188	0.812
Hoj404(E19)	cultivated	11.1	0.125	0.875
Hoj453(2Ñ)	cultivated	11.1	0.15	0.85

Methods S1 Nonlinear function explaining environmental influence on reproductive pathways

In order to better understand the ecological influence on reproductive modes and to model its possible responses, a nonlinear function for the observed expression of meiotic and apomictic pathways and the MDR was formulated. The nonlinear equation best explaining our results takes the form of an exponential increase/decay with a horizontal asymptote. For apomixis it can be written as

$$A_{(d)} = A_m + A_0 \cdot e^{-k(d - d_0)}$$

Where, A_m is the minimum AES%, A_0 is the maximum AES%, k is the gradient constant, d is diurnal variation (MDR) and the d_0 is the temperature at which AES% is 100%. The values obtained from the grid search (see Materials and Methods) were, $A_m = 30\%$, $k = 0.21$ and $d_0 = 7.8$; A_0 was assumed to be 100 as it is the maximum theoretical AES% possible. Therefore, the equation can be written as

$$A_{(d)} = 30 + 100 \cdot e^{(-0.21(d-7.8))} \quad (\text{see Figure 4})$$

The same procedure was followed for the seed data. However, all of our attempts to formulate a non-linear model equation failed to converge, presumably due to the lack of data points along the MDR zones. From the similarity of the trend lines observed for the ovule stage between the GLM and non-linear model we can assume a similar non-linear behavior for the seed stage respect to MDR.